

Published in final edited form as:

Cancer Res. 2013 May 15; 73(10): 3145–3154. doi:10.1158/0008-5472.CAN-13-0011.

β 1 Integrin Targeting Potentiates Antiangiogenic Therapy and Inhibits the Growth of Bevacizumab-Resistant Glioblastoma

W. Shawn Carbonell¹, Michael DeLay¹, Arman Jahangiri¹, Catherine C. Park², and Manish K. Aghi¹

¹Department of Neurosurgery, University of California, San Francisco, San Francisco, California

²Department of Radiation Oncology, University of California, San Francisco, San Francisco, California

Abstract

Antiangiogenic therapies like bevacizumab offer promise for cancer treatment, but acquired resistance, which often includes an aggressive mesenchymal phenotype, can limit the use of these agents. Upregulation of β 1 integrin (ITGB1) occurs in some bevacizumab-resistant glioblastomas (BRG) whereby, mediating tumor–microenvironment interactions, we hypothesized that it may mediate a mesenchymal-type resistance to antiangiogenic therapy. Immunostaining analyses of β 1 integrin and its downstream effector kinase FAK revealed upregulation in 75% and 86% of BRGs, respectively, compared with pretreatment paired specimens. Furthermore, flow cytometry revealed eight-fold more β 1 integrin in primary BRG cells compared with cells from bevacizumab-naïve glioblastomas (BNG). Fluorescence recovery after photobleaching of cells engineered to express a β 1-GFP fusion protein indicated that the mobile β 1 integrin fraction was doubled, and half-life of β 1 integrin turnover in focal adhesions was reduced markedly in BRG cells compared with bevacizumab-responsive glioblastoma multiforme cells. Hypoxia, which was increased with acquisition of bevacizumab resistance, was associated with increased β 1 integrin expression in cultured BNG cells. BRGs displayed an aggressive mesenchymal-like phenotype *in vitro*. We

© 2013 American Association for Cancer Research.

Corresponding Author: W. Shawn Carbonell, University of California at San Francisco, 505 Parnassus Avenue, Room M779, San Francisco, CA 94143. Phone: 415-666-2391; Fax: 415-901-1095; shawn@oncosynergy.com.

M. DeLay and A. Jahangiri contributed equally to this work.

Current address for W.S. Carbonell: OncoSynergy, Inc., San Francisco, CA 94158.

Note: Supplementary data for this article are available at Cancer Research Online (<http://cancerres.aacrjournals.org/>).

Disclosure of Potential Conflicts of Interest

W. Shawn Carbonell is employed as a cofounder, President, and CEO, and has ownership interest (including patents) in OncoSynergy, Inc. C.C. Park has ownership interest (including patents) in OncoSynergy Ltd. M.K. Aghi is employed as a scientific advisory board member/shareholder, has ownership interest (including patents), and is a consultant/advisory board member of OncoSynergy. No potential conflicts of interest were disclosed by the other authors.

Authors' Contributions

Conception and design: W.S. Carbonell, M. DeLay, A. Jahangiri, C.C. Park, M.K. Aghi

Development of methodology: W.S. Carbonell, M. DeLay, A. Jahangiri, M.K. Aghi

Acquisition of data (provided animals, acquired and managed patients, provided facilities, etc.): W.S. Carbonell, M. DeLay, A. Jahangiri, M.K. Aghi

Analysis and interpretation of data (e.g., statistical analysis, biostatistics, computational analysis): W.S. Carbonell, M. DeLay, M.K. Aghi

Writing, review, and/or revision of the manuscript: W.S. Carbonell, M. DeLay, A. Jahangiri, C.C. Park, M.K. Aghi

Administrative, technical, or material support (i.e., reporting or organizing data, constructing databases): M.K. Aghi

Study supervision: W.S. Carbonell, M.K. Aghi

found that growth of BRG xenograft tumors was attenuated by the $\beta 1$ antibody, OS2966, allowing a 20-fold dose reduction of bevacizumab per cycle in this model. Intracranial delivery of OS2966 through osmotic pumps over 28 days increased tumor cell apoptosis, decreased tumor cell invasiveness, and blunted the mesenchymal morphology of tumor cells. We concluded that $\beta 1$ integrin upregulation in BRGs likely reflects an onset of hypoxia caused by antiangiogenic therapy, and that $\beta 1$ inhibition is well tolerated *in vivo* as a tractable strategy to disrupt resistance to this therapy.

Introduction

Glioblastoma multiforme is the most common malignant brain tumor in adults, with a median survival close to 1 year (1). To date, only 3 drugs have been approved by the U.S. Food and Drug Administration for glioblastoma treatment, including, most recently, bevacizumab (Avastin; Genentech) in 2009 (2). Despite improvements in clinical metrics with bevacizumab including cognitive benefits and reduction of steroid use (3), 40% of treated patients developed acquired resistance in phase II trials (4). Thus, as has been the case with other cancers treated with antiangiogenic therapy, the promise of antiangiogenesis in glioblastoma remains unfulfilled in part due to acquired resistance.

Integrins are cell-adhesion molecules that mechanosense the microenvironment and elicit extracellular-matrix (ECM)-induced signaling in both normal and pathologic states such as inflammation and cancer. Importantly, integrins lie at the interface of the cell and microenvironment, playing a key role in tumor progression and regulating growth and survival pathways. Upregulation of integrins has been associated with epithelial malignancies (5), particularly during invasion, metastasis, and angiogenesis (6, 7). There is growing evidence for the role of aberrantly expressed integrins in glioblastoma pathophysiology (8). $\beta 3$ and $\beta 5$ integrins have been implicated in angiogenesis, and several approaches targeting these molecules are under investigation in the clinic (9). $\beta 1$ integrins, which coordinate much broader functional activities such as inflammation, proliferation, adhesion, and invasion, have recently been implicated in therapeutic resistance in multiple solid cancer models (10–13) and hematopoietic malignancies (14, 15). Importantly, this $\beta 1$ integrin-mediated resistance is thought to occur at the level of the tumor cells themselves. $\beta 1$ integrin also has important functions during tumor vascularization such as VEGF-dependent (16) and VEGF-independent angiogenesis by promoting endothelial cell migration (17). Notably, as shown in glioblastoma models (18–20), we found that bevacizumab causes U87MG, a commonly studied glioblastoma cell line, to grow more invasively (Supplementary Fig. S1A), and orthotopic bevacizumab-resistant glioblastoma (BRG) xenografts infiltrate the brain via vessel co-option, which has been shown to require $\beta 1$ integrins (21), whereas bevacizumab-naïve glioblastoma (BNG) xenografts remain well circumscribed (Supplementary Fig. S1B; ref. 22). This evidence, when taken together, led us to investigate the novel hypothesis that $\beta 1$ integrin drives resistance to antiangiogenic therapy by promoting multiple mechanisms at the interface of tumor cells and the microenvironment.

Materials and Methods

Collection and analysis of human clinical specimens

Human specimens were obtained from the University of California, San Francisco (UCSF; San Francisco, CA) Brain Tumor Tissue Bank (22). Fluorescence immunohistochemistry of human paraffin-embedded tissues for β 1 integrin (ab52971; Abcam), CA9 (Novus Biologicals), FAK^{Y397} (ab4803; Abcam), GFAP (ab4674; Abcam), and laminin (ab14055; Abcam) was conducted with either standard indirect or tyramide signal amplification (PerkinElmer) as described (21) following standard citrate buffer (Abcam) antigen retrieval.

Cells and cell lines

U87MG, MDA-MB-231, and SW-1080 cell lines were obtained from and authenticated by American Type Culture Collection and passed in less than 6 months. Cells were maintained in Dulbecco's Modified Eagle Medium (DMEM) supplemented with 10% FBS, nonessential amino acids (NEAA), and antibiotics. The bevacizumab-resistant primary glioblastoma cells, SF7796 and SF8106, and the bevacizumab-naïve primary glioblastoma cells, SF7996 and SF8244, were obtained and grown as described (22). Bevacizumab-resistant (BRG1, BRG2, and BRG3) and bevacizumab-naïve (N1, N2, and N3) cell lines were derived from fresh clinical resection specimens at UCSF as described (22) and were propagated in 50% to 50% DMEM/F-12 with 10% FBS, NEAA, and antibiotics. Primary SF8106 and SF7796 glioma cultures were transfected with the pFB-Neo Retroviral Vector (Agilent) containing a cDNA expressing the β 1-GFP fusion protein (gift of Martin Humphries; University of Manchester, UK), followed by selection in 5 μ g/mL geneticin (Gibco), as described (23). Experimental hypoxia was induced by growth in 1% oxygen as described (24).

Short hairpin RNA-mediated integrin knockdown

U87MG, BRG2, and BRG3 cells were infected with short hairpin RNA (shRNA) lentiviral particles (Santa Cruz Biotechnology) targeting β 3 integrin (sc-63292-V), β 1 integrin (sc-35674-V), or vector control (shCTRL, sc-108084) per manufacturer's protocol. After 48 hours, subcultured cells were selected in 1 μ g/mL puromycin for 1 week.

Flow cytometry

Cells were trypsinized in 0.25% trypsin with EDTA, counted, resuspended in PBS at 10^6 cells/mL, and kept on ice. Cell surface β 1 integrin was labeled with anti- β 1 integrin antibodies OS2966 (OncoSynergy, Inc.), CD29 (Clone TS-2/16, BioLegend), or CD29 (Clone K20, BD). Cell surface c-MET was detected with Clone 95106 monoclonal antibody (mAb; R&D Systems). Flow cytometry was conducted with a BD FACS Calibur II machine, and data were analyzed using FlowJo software (Tree Star, Inc.).

Western blot analysis

Western blots were conducted as described previously (25), using primary antibody to β 1 integrin (Biolegend; Abcam) along with α V, α 5, α 4, and β 3 antibodies (Cell Signaling).

Fluorescence recovery after photobleaching

SF8106/B1-GFP and SF7996/B1-GFP cells were seeded at 10,000 cells per well on chambered coverglass (Fisher), which had been coated overnight with 10 µg/mL fibronectin (Sigma-Aldrich). Individual cells were analyzed on a Zeiss LSM 510 NLO Meta confocal microscope. Target-bleach regions were normalized to background observational bleaching. Images were collected every 30 seconds until fluorescence recovery plateau. Fractional fluorescence recovery and half-time of recovery were calculated as described (26).

Dynamic *in vitro* assays and timelapse microscopy

Adhesion assays were conducted as described (21) on plates coated with 10 µg/mL fibronectin (Sigma). Scratch assays were conducted as described (27) on plates coated with 10 µg/mL fibronectin. Cell spreading assays were conducted by plating 10⁵ cells on a 30-mm dish coated with 10 µg/mL fibronectin. Time-lapse phase-contrast microscopy was conducted as described (21) with a Zeiss Observer Z1 inverted microscope with an AxioCam MRm and accompanying AxioVision 4.8 software. Briefly, 30-mm dishes were placed upon a heated stage adapter (Stable Z with heated lid, Bioprotechs), and images were captured every 90 to 180 seconds for up to 24 hours. Media were covered with sterile embryo-tested mineral oil (Sigma).

Cell adhesion was quantified as described (21). Cell spreading was quantitated as cell area (measured hourly) and percentage of spread cells per high-power field. For cell area, all whole cells in a ×40 field were measured manually in ImageJ (NIH) at time zero and every hour for 5 hours. Means were calculated at each timepoint and compared. The percentage of spread cells per ×40 field was similarly calculated hourly (not including time zero) for 12 hours. Cell migration and dendricity factor for cell shape were measured as described (22, 28).

Cell proliferation

Bromodeoxyuridine (BrdU) immunofluorescence was conducted by incubating cells in 10 µmol/L BrdU (Sigma) for 1 hour in complete media followed by fixation in 1% paraformaldehyde. Cells were permeated in 0.1% Triton-X100 (Sigma) in PBS on ice for 5 minutes followed by incubation in biotinylated sheep anti-BrdU antibody (ab2284, Abcam) overnight at 4°C. Following PBS washes, cells were incubated with streptavidin-Alexa555 (Invitrogen) and coverslipped with VectaShield mounting medium with DAPI (VectorLabs). BrdU-positive cells per high-power field were counted in three 40× fields per well, 3 wells per experiment with repeats.

Tumor spheroid assays

Aggregation assays were conducted by suspending tumor cells in PBS on ice for 15 minutes. To visualize β1 integrin, cells were incubated with Alexa 647 conjugated anti-CD29 (clone TS-2/16) for 15 minutes, spun down, and rinsed. Cell growth in acidified media was conducted as described (29). Spheroidal growth assays were conducted in 6-well ultra-low adhesion plates (CoStar) with standard conditions for growth of neuro-spheres (29) for 3 to 5 days. Spheroid dissolution assays were conducted by plating spheroids on culture dishes

coated with 10 $\mu\text{g}/\text{mL}$ of bovine serum albumin (BSA) control, fibronectin, laminin, or collagen type IV (all ECM from Sigma) for 5 to 7 days.

Xenograft studies

Animal procedures were approved by the UCSF Institutional Animal Care and Use Committee (IACUC). A total of 10^5 to 10^6 cells were injected s.c. or 10^5 cells were injected stereotactically into the right caudate (orthotopic model) of 5- to 8-week-old female athymic mice. Mice were randomized into treatment groups after tumors were established (mean s.c. volume = 40–60 mm^3 or 10 days after intracranial implantation). Bevacizumab and human immunoglobulin G (IgG) control (Sigma) were administered at 10 mg/kg intra-peritoneally (i.p.) twice weekly. Inhibitory anti- $\beta 1$ integrin mAb OS2966 or control IgG was administered at 1, 5, or 10 mg/kg i.p. twice weekly. For orthotopic studies, OS2966 or IgG (160 μg total) was delivered intratumorally over 28 days via rigid cannula connected to Model 1004 osmotic pumps (Alzet) implanted s.c. between the scapulae. Subcutaneous tumors were measured with calipers 1 to 2 times weekly, with volume calculated as described (24). Treatment continued until mice had to be sacrificed per IACUC criteria (e.g., 2.1-cm maximal dimension, cutaneous ulceration, or symptoms) or study end.

Tissue preparation and immunohistochemistry

Mice were sacrificed and tissue collected and prepared as described (21). Cryostat sections (20–30 μm in size) were collected and mounted directly on slides and were processed for immunohistochemistry as described (21). For TUNEL staining, the TMR red *In Situ* Cell Death Detection Kit (Roche) was used. Immunohistochemistry was conducted using antibodies against $\beta 1$ (Abcam), laminin (Abcam), GFAP (Millipore), and GLUT-1 (Millipore). Collagen IV immunostaining was described previously (25).

Statistical analyses

Student *t* test was used for parametric comparisons between paired variables. The Mann–Whitney *U* test was used for nonparametric pairwise comparisons. Multivariate analyses were done with ANOVA with *post hoc* Dunnett (most analyses) or Bonferroni tests (e.g., xenograft studies) as appropriate. $P < 0.05$ was deemed statistically significant.

Results

Upregulation of $\beta 1$ integrin after acquired resistance to bevacizumab

We recently reported by microarray analysis and confirmatory PCR that transcription of $\beta 1$ integrin was upregulated in glioblastomas exhibiting the nonenhancing infiltrative pattern of growth that is viewed as unique to bevacizumab resistance (22). To further verify this result, we conducted immunohistochemistry on BRGs and their paired pretreatment specimens and found increased $\beta 1$ integrin in 9 of 12 cases (75%, Fig. 1A). This increased immunoreactivity was observed in both angiogenic blood vessels (Fig. 1A, arrows) and tumor cells (Fig. 1B). Consistent with *bona fide* integrin signaling, we found increased phosphorylated focal adhesion kinase staining in tumor cells in 6 of 7 BRG cases compared with pretreatment, with staining tending to be close to ECM (Fig. 1C; refs. 30, 31). Furthermore, $\beta 1$ integrin was increased in primary cells from BRG clinical specimens

compared with primary cultures established from BNG specimens by fluorescence-activated cell sorting ($P < 0.05$; Fig. 1D). To rule out contributions from patient variability among clinically derived samples that could affect integrin expression, we experimentally derived a bevacizumab-resistant xenograft from U87MG (U87-BEV; ref. 25). Screening of integrin expression revealed that U87-BEV showed significantly higher expression of $\beta 1$ integrin, along with αV and $\alpha 5$ integrins, 2 potential $\beta 1$ heterodimer partners, which interact to promote fibronectin binding (32), compared with U87-IGG, a control line treated only with IgG (Supplementary Fig. S2A and S2B).

Because the percentage of integrin that is mobile and the turnover of this mobile integrin in focal adhesions sustains integrin signaling, we engineered BRG and BNG cells to express a $\beta 1$ -GFP fusion protein and used fluorescence recovery after photobleaching (FRAP) to measure integrin turnover in focal adhesions (26). We found 2-fold faster $\beta 1$ integrin turnover in focal adhesions and double the mobile fraction of $\beta 1$ integrin in bevacizumab-resistant SF8106 cells than in bevacizumab-responsive SF7996 cells (Fig. 1E and Supplementary Fig. S2C). Thus, compared with BNG cells, bevacizumab-resistant cells exhibited more mobile $\beta 1$ integrin, reflective of reduced cellular membrane barriers to $\beta 1$ integrin mobility in these cells and more rapid turnover of $\beta 1$ integrin in focal adhesions.

To verify the functional relevance of increased $\beta 1$ integrin in glioblastoma cells, we conducted cell adhesion assays and found significantly greater adhesion to ECM in BRGs compared with classic glioblastoma lines and even the highly adhesive MDA-MB-231 human breast adenocarcinoma, which served as a positive control (Fig. 1F). Thus, the $\beta 1$ integrin subunit is functionally upregulated in glioblastoma after acquired bevacizumab resistance.

Hypoxia associated with high $\beta 1$ integrin expression in glioblastoma cells

Hypoxia is a common cellular stress, particularly in the setting of fast-growing cancers and variably during the course of antiangiogenic therapy. Hypoxia upregulates $\beta 1$ integrin expression in the setting of wound healing via hypoxia-inducible factor-1 α (HIF-1 α)–stimulated $\beta 1$ transcription (33). We showed nearly 80% more CA9 staining after bevacizumab resistance as compared with before, with areas of CA9 staining corresponding with high $\beta 1$ integrin expression in patient glioblastoma specimens (Supplementary Fig. S3A). To verify that antiangiogenic therapy acutely increases $\beta 1$ integrin expression in growing tumors *in vivo*, we stained glioblastoma tumors from mice taken within days of the last bevacizumab treatment. Striking $\beta 1$ integrin immunoreactivity was observed in the treated tumors compared with controls, particularly in the hypoxic tumor core (Supplementary Fig. S3B). To confirm this mechanism, we cultured U87MG cells for 6 to 48 hours in 1% oxygen to simulate microenvironmental hypoxia. We observed a significant increase in $\beta 1$ integrin expression in glioma cells *in vitro* (Supplementary Fig. S3C). This was a rapid and reversible cellular response, which we also showed in primary human glioblastoma cells and breast and colorectal carcinoma cells (Supplementary Fig. S3D). Therefore it is likely that hypoxia contributes to $\beta 1$ integrin upregulation during bevacizumab therapy, thus promoting mechanisms of survival and evasion.

β 1 integrin inhibition attenuates mesenchymal phenotype and function of BRG cells

To further establish a functional role for β 1 integrin in the malignant phenotype of bevacizumab glioblastoma cells, we established several clones of the BRG3 line expressing shRNA-targeting β 1 integrin (shBETA1) and shRNA-targeting control sequences (shCTRL; Supplementary Fig. S4A–S4D). An epithelioid morphologic shift, including polygonal shape and tendency for growth in sheets, was observed in the shBETA1 clones compared with shCTRL cells (Supplementary Fig. S5A). Indeed, individual cell size as measured by cell area was significantly increased in the shBETA1 clones compared with shCTRL (Supplementary Fig. S5B). In addition, dendricity factor, a unitless measure of cell shape, confirmed mesenchymal morphology in the shCTRL cells compared with more epithelioid morphology in the shBETA1 clones (Supplementary Fig. S5C). To verify functional impairment of mesenchymal phenotype, we examined the knockdown cells in various static and dynamic *in vitro* assays. As hypothesized, BRG3-shBETA1 clones showed significantly decreased capacity for mesenchymal functions, including adhesion (Fig. 2A), cell spreading (Fig. 2B and C and Supplementary Movie S1), and migration (Fig. 2D and E and Supplementary Movie S2) on ECM compared with BRG3-shCTRL cells. Furthermore, bevacizumab-naïve cells showed epithelial-like migration with broad lamellipodia (Supplementary Movie S3) in contrast with the saltatory mesenchymal-type migration seen in the BRG3 line. In addition, *in vitro* proliferation (Fig. 2F) was significantly attenuated in the BRG3-shBETA1 clones compared with BRG3-shCTRL cells. This effect of β 1 integrin knockdown in the BRG3 line on cell growth *in vitro* was determined to be cytostatic, rather than cytotoxic (Supplementary Fig. S5D). Similar results on adhesion, migration, and proliferation were found when the BRG3 line was treated with the inhibitory β 1 integrin mAb, OS2966 (Supplementary Fig. S6A and S6B and Supplementary Movie S4). Thus, β 1 integrin is important for multiple tumor cell functions implicated in antiangiogenic therapy evasion, including persistent proliferation and mesenchymal phenotype.

Spheroidal growth is impaired by β 1 integrin inhibition

Microenvironmental hypoxia (34) and acidification (29) are 2 suspected consequences of antiangiogenic therapy, and both activate HIF-1 α and HIF-2 α expression. Both hypoxia-associated factors have also been linked to malignant stem-like phenotypes in glioblastoma cells including *in vitro* spheroid formation. Indeed, freshly isolated bevacizumab-resistant U87-BEV cells are more highly prone to spheroid formation *in vitro* compared with the control U87-IGG line under normal culture conditions (Supplementary Fig. S7A). Implantation of glioblastoma spheroids has been shown to be associated with decreased survival in orthotopic xenograft studies compared with control cells (29). Importantly, we observed that acutely dissociated BRG1 and BRG3 glioblastoma cells in suspension show the highest β 1 integrin expression at cell–cell contacts (Fig. 3A). Therefore, to investigate a potential role for β 1 integrins in glioblastoma spheroid formation, we cultured U87MG cells under acidic stress. Spheroid formation in acidic media was attenuated in U87-shBETA1 (Supplementary Fig. S7B) cells compared with control U87-shCONTROL cells (Fig. 3B). Similar results were obtained with parental U87MG cells treated with an inhibitory β 1 integrin antibody (Supplementary Fig. S7C). To more directly study spheroid formation, we grew glioblastoma cells in suspension in nonadherent plates. U87 cells with stable

knockdown of $\beta 1$ integrin (U87-shBETA1) showed significantly smaller spheroid diameters than control U87-shCONTROL cells (Fig. 3C). The same result was found in knockdown clones from the clinically derived BRG3 line (Fig. 3D). Furthermore, confirming the role of $\beta 1$ integrins in spheroidal maintenance, we showed dissolution of glioblastoma spheroids when plated on classic $\beta 1$ integrin ECM substrates, particularly fibronectin (Fig. 3E). Thus, the $\beta 1$ integrin subunit is intimately involved in cell–cell interactions and malignant spheroidal growth in glioma cells *in vitro*, a phenotype that has been associated with increased malignancy *in vivo*.

$\beta 1$ integrin inhibition prevents BRG growth *in vivo*

To test the role of $\beta 1$ integrin in glioma growth and bevacizumab resistance *in vivo*, we used several glioma cell models in athymic mice. First, we showed attenuation of tumor growth in the BRG2 and BRG3 lines after stable knockdown of $\beta 1$ integrin (polyclonal, approximately 70% knockdown). In both cases, tumor growth was significantly impaired in the shBETA1 cells compared with shCTRL cells (Fig. 4A and B). We then inoculated mice with clones of BRG3 that had more than 90% knockdown of $\beta 1$ integrin. Consistent with a gene–dosage effect, we showed complete prevention of *in vivo* tumor growth for 6 months (Fig. 4C). Thus, $\beta 1$ integrin inhibition overcomes growth of both BNG and BRG cells *in vivo*.

To provide proof-of-concept for a clinically relevant treatment modality, we tested a therapeutic antibody approach in a glioma xenograft model. Mice inoculated with the BRG3 cell line were systemically treated with inhibitory $\beta 1$ integrin monoclonal antibodies (OS2966) at 2 doses. Both groups of treated mice had significantly smaller tumors than mice treated with 5 mg/kg of control IgG (Fig. 4D and E). Strikingly, 56% (5/9) of mice with BRG3 tumors treated with 5 mg/kg OS2966 showed complete tumor regression after 8 weeks of treatment. We observed apoptosis on histology in the treated group but not in the IgG control (Fig. 4F). Finally, to verify the above findings in an orthotopic model, we stereotactically implanted BRG3 cells into the striatum of mice. Ten days after inoculation, we implanted cannulae through the same burr hole for chronic intratumoral delivery of either OS2966 or IgG control via s.c. osmotic pumps that provided antibody delivery for 28 days. Successful tumoral delivery of antibodies was verified with immunofluorescence detection of OS2966 in horizontal brain sections (Supplementary Fig. S8). BRG3 cells in the control condition formed highly invasive tumors, and 55.2% \pm 11% of invading cells were associated with the neurovasculature according to GLUT-1 immunoreactivity for endothelial cells (Fig. 5A). OS2966 treatment resulted in complete regression of tumors (3/3 mice) as supported by massive induction of tumor cell apoptosis on TUNEL staining (Fig. 5B). Finally, OS2966 treatment inhibited striatal invasion as shown by number of invading cells per section (Fig. 5C) and invasion distance (Fig. 5D). Accordingly, OS2966 treatment seemed to directly affect invasive morphology of tumor cells (Fig. 5E). Thus, blockade of $\beta 1$ integrin function with inhibitory monoclonal antibodies attenuates growth of a recurrent bevacizumab-resistant glioma line *in vivo*.

β 1 integrin inhibition potentiates bevacizumab treatment

Not all patients respond to bevacizumab, and significant morbidity is associated with its long-term use. Therefore, there is clinical need for a novel therapeutic approach to improve response rates, prevent resistance, and potentially reduce the necessary dose of bevacizumab. Toward this end, full-dose combination therapy of OS2966 with bevacizumab was attempted in the U87MG subcutaneous xenograft model in 2 separate investigations. However, both studies had to be halted before their endpoints due to rapid cutaneous tumor ulceration in 100% (5/5 and 10/10 mice, respectively) of the combination therapy animals by the third week of treatment. These findings are suggestive of synergy between OS2966 and bevacizumab. To explore this question further, we hypothesized that the addition of OS2966 alternating with low-dose bevacizumab would enhance efficacy in U87MG xenografts (Fig. 6A). Indeed, alternating OS2966 and bevacizumab at 1 mg/kg, each was equivalent to a biweekly standard dose of bevacizumab (10 mg/kg) in this setting (Fig. 6B). Furthermore, the percentage of animals with complete regression of tumors was nearly equivalent, with 44% (4/9) of mice in the alternating low-dose group compared with 56% (5/9) of mice in the standard dose group. Thus, consistent with its multiple roles in promoting therapeutic resistance, β 1 integrin is potentially a promising adjunct target in combination with antiangiogenic therapies, including bevacizumab.

Discussion

Our data show for the first time that resistance to anti-angiogenic therapy is associated with increased expression of β 1 integrin as well as increased mobility of β 1 integrin and increased turnover of β 1 integrin in focal adhesions. We also showed that resistance to antiangiogenic therapy can be overcome by targeting tumor cell interactions with the glioma microenvironment via β 1 integrin inhibition. In contrast to approaches that target a specific integrin–ligand interaction (e.g., natalizumab, which targets α 4 integrin, blocking the ability of α 4 β 1 or α 4 β 7 to bind VCAM-1), a single drug targeting β 1 would inhibit the ability of tumor cells to bind a spectrum of ECM ligands like fibronectin, collagen IV, and laminin, each of which we found to be upregulated in BRGs (22). This approach could potentially be applied more broadly in several medical indications. Inhibition of β 1 integrin overcomes resistance to antiangiogenesis therapy via multiple potential mechanisms: (i) preventing vessel cooption (and/or growth/invasion upon any classical ECM substrate; ref. 21); (ii) reducing viability of tumor cells after insults (35); (ii) directly inhibiting tumor cell proliferation; (iii) directly inhibiting the vascularization process (36); and (iv) inhibiting the aggressive mesenchymal phenotype, including spheroidal growth. In addition, β 1 integrin inhibition alternating with bevacizumab can reduce the necessary dose of antiangiogenic agent, thus potentially reducing drug-related morbidity.

It is tempting to speculate that because breast and other cancer cells also respond to insults with an increase in β 1 integrin expression (e.g., Supplementary Fig. S3D), this approach may be applicable for the treatment of a wide variety of high-grade and/or treatment-refractory adenocarcinomas. This hypothesis warrants further study. Indeed, β 1 integrin has proved to be a viable oncological target in animal models of solid and blood-borne cancers for multiple processes, including (i) prevention and growth of metastasis (37); (ii)

overcoming resistance to radiation (35) and chemotherapy (38–42); and (iii) inhibition of local carcinoma spread. In addition, $\beta 1$ integrin upregulation has been shown to be prognostic for breast (38, 43), lung (44), and pancreatic (37) cancers.

A limitation of the current study is the inability to directly study the effect of antiangiogenesis mechanistically *in vitro*. Bevacizumab acts at the endothelium, causing ischemia and other tissue-level processes, which cannot be accurately modeled with isolated tumor cells or cocultures. Therefore, the spectrum of adaptations to antiangiogenic therapy cannot currently be reliably assessed *in vitro*. We have addressed this limitation with a multimodal approach using clinical specimens and their cellular derivatives in surrogate *in vitro* assays (e.g., hypoxia, acidified media) and relevant preclinical murine models. Of note, these murine models were generated by treating tumors with bevacizumab, which targets human, not murine VEGF, and would therefore target only tumor cells rather than stromal cells. However, we have found that bevacizumab is equally effective in xenograft treatment as an agent-targeting mouse and human VEGF (personal communication, C. David James, Department of Neurological Surgery, University of California, San Francisco, CA; 2008).

The orthotopic model with bevacizumab-resistant BRG3 cells revealed several important findings. First, we confirmed that parenchymal invasion of bevacizumab-resistant glioma cells occurs primarily via vessel cooption. Second, OS2966 delivered via osmotic pump nearly completely abolished invasion of BRG3 cells. In addition, inhibition of $\beta 1$ integrin in these studies resulted in tumor cell apoptosis and disrupted tumor mass formation. Because of the finite life of the osmotic pumps, survival studies were not possible; however, the results provide solid proof-of-concept for intracranial delivery of OS2966 as a treatment for BRG via modalities like convection-enhanced delivery, which would enable more high-flow intratumoral infusion of OS2966 (45). Although local delivery of $\beta 1$ integrin-targeted therapy would be appealing by increasing local concentrations of the therapeutic agent and minimizing systemic exposure, it should be noted that an antibody targeting $\beta 1$ integrin was nontoxic when systemically delivered in our studies and other studies (35).

Although we have shown that alternating low doses of $\beta 1$ integrin inhibition with bevacizumab can reduce the necessary weekly dose of bevacizumab by 20 times and can inhibit growth of bevacizumab-resistant glioma cells, the question remains whether alternate or combination therapy can attenuate development of resistance to bevacizumab over longer treatment periods. To define the full potential of our approach in the clinic will require exploring various dosing schedules and combinations *in vivo*. Still, our data suggest that $\beta 1$ integrin inhibition as monotherapy for BRG or combined with bevacizumab to reduce the risk of resistance are promising therapeutic strategies.

Supplementary Material

Refer to Web version on PubMed Central for supplementary material.

Acknowledgments

The authors thank Rick Horwitz for helpful discussion.

Grant Support

This work was supported by funding from the James S. McDonnell Foundation, the American Cancer Society (ACS), and NIH 5K02NS64167-2 (M.K. Aghi); the Howard Hughes Medical Institute (A. Jahangiri); and NIH grant 1R01CA124891 and ACS RSG-07-1110-01-CCE (C.C. Park).

References

1. Stupp R, Dietrich PY, Ostermann Kraljevic S, Pica A, Maillard I, Maeder P, et al. Promising survival for patients with newly diagnosed glioblastoma multiforme treated with concomitant radiation plus temozolomide followed by adjuvant temozolomide. *J Clin Oncol.* 2002; 20:1375–82. [PubMed: 11870182]
2. Kreisl TN, Kim L, Moore K, Duic P, Royce C, Stroud I, et al. Phase II trial of single-agent bevacizumab followed by bevacizumab plus irinotecan at tumor progression in recurrent glioblastoma. *J Clin Oncol.* 2009; 27:740–5. [PubMed: 19114704]
3. Kienast Y, Winkler F. Therapy and prophylaxis of brain metastases. *Expert Rev Anticancer Ther.* 2010; 10:1763–77. [PubMed: 21080803]
4. Vredenburgh JJ, Desjardins A, Herndon JE II, Dowell JM, Reardon DA, Quinn JA, et al. Phase II trial of bevacizumab and irinotecan in recurrent malignant glioma. *Clin Cancer Res.* 2007; 13:1253–9. [PubMed: 17317837]
5. Gotzmann J, Mikula M, Eger A, Schulte-Hermann R, Foisner R, Beug H, et al. Molecular aspects of epithelial cell plasticity: implications for local tumor invasion and metastasis. *Mutat Res.* 2004; 566:9–20. [PubMed: 14706509]
6. Foubert P, Varner JA. Integrins in tumor angiogenesis and lymphangiogenesis. *Methods Mol Biol.* 2012; 757:471–86. [PubMed: 21909928]
7. Tchaicha JH, Reyes SB, Shin J, Hossain MG, Lang FF, McCarty JH. Glioblastoma angiogenesis and tumor cell invasiveness are differentially regulated by $\beta 8$ integrin. *Cancer Res.* 2011; 71:6371–81. [PubMed: 21859829]
8. Reardon DA, Nabors LB, Stupp R, Mikkelsen T. Cilengitide: an integrin-targeting arginine-glycine-aspartic acid peptide with promising activity for glioblastoma multiforme. *Expert Opin Investig Drugs.* 2008; 17:1225–35.
9. Tucker GC. Integrins: molecular targets in cancer therapy. *Curr Oncol Rep.* 2006; 8:96–103. [PubMed: 16507218]
10. Cordes N, Park CC. beta1 integrin as a molecular therapeutic target. *Int J Radiat Biol.* 2007; 83:753–60. [PubMed: 18058364]
11. Desgrosellier JS, Cheresh DA. Integrins in cancer: biological implications and therapeutic opportunities. *Nat Rev Cancer.* 2010; 10:9–22. [PubMed: 20029421]
12. Sethi T, Rintoul RC, Moore SM, MacKinnon AC, Salter D, Choo C, et al. Extracellular matrix proteins protect small cell lung cancer cells against apoptosis: a mechanism for small cell lung cancer growth and drug resistance *in vivo*. *Nat Med.* 1999; 5:662–8. [PubMed: 10371505]
13. Meads MB, Gatenby RA, Dalton WS. Environment-mediated drug resistance: a major contributor to minimal residual disease. *Nat Rev Cancer.* 2009; 9:665–74. [PubMed: 19693095]
14. Hazlehurst LA, Landowski TH, Dalton WS. Role of the tumor micro-environment in mediating *de novo* resistance to drugs and physiological mediators of cell death. *Oncogene.* 2003; 22:7396–402. [PubMed: 14576847]
15. Matsunaga T, Fukai F, Miura S, Nakane Y, Owaki T, Kodama H, et al. Combination therapy of an anticancer drug with the FNIII14 peptide of fibronectin effectively overcomes cell adhesion-mediated drug resistance of acute myelogenous leukemia. *Leukemia.* 2008; 22:353–60. [PubMed: 17972943]
16. Leenders WP, Kusters B, Verrijp K, Maass C, Wesseling P, Heerschap A, et al. Antiangiogenic therapy of cerebral melanoma metastases results in sustained tumor progression via vessel co-option. *Clin Cancer Res.* 2004; 10:6222–30. [PubMed: 15448011]
17. Azam F, Mehta S, Harris AL. Mechanisms of resistance to antiangiogenesis therapy. *Eur J Cancer.* 2010; 46:1323–32. [PubMed: 20236818]

18. Bergers G, Hanahan D. Modes of resistance to anti-angiogenic therapy. *Nat Rev Cancer*. 2008; 8:592–603. [PubMed: 18650835]
19. de Groot JF, Fuller G, Kumar AJ, Piao Y, Eterovic K, Ji Y, et al. Tumor invasion after treatment of glioblastoma with bevacizumab: radiographic and pathologic correlation in humans and mice. *Neuro Oncol*. 2010; 12:233–42. [PubMed: 20167811]
20. Janouskova H, Maglott A, Leger DY, Bossert C, Noulet F, Guerin E, et al. Integrin $\alpha 5\beta 1$ plays a critical role in resistance to temozolomide by interfering with the p53 pathway in high grade glioma. *Cancer Res*. 2012; 72:3463–70. [PubMed: 22593187]
21. Carbonell WS, Ansorge O, Sibson N, Muschel R. The vascular basement membrane as “soil” in brain metastasis. *PLoS ONE*. 2009; 4:e5857. [PubMed: 19516901]
22. De Lay M, Jahangiri A, Carbonell WS, Hu YL, Tsao S, Tom MW, et al. Microarray analysis verifies two distinct phenotypes of glioblastomas resistant to anti-angiogenic therapy. *Clin Cancer Res*. 2012; 18:2930–42. [PubMed: 22472177]
23. Parsons M, Messent AJ, Humphries JD, Deakin NO, Humphries MJ. Quantification of integrin receptor agonism by fluorescence lifetime imaging. *J Cell Sci*. 2008; 121:265–71. [PubMed: 18216331]
24. Hu YL, Delay M, Jahangiri A, Molinaro AM, Rose SD, Carbonell WS, et al. Hypoxia-induced autophagy promotes tumor cell survival and adaptation to antiangiogenic treatment in glioblastoma. *Cancer Res*. 2012; 72:1773–83. [PubMed: 22447568]
25. Jahangiri A, De Lay M, Miller LM, Carbonell WS, Hu YL, Lu K, et al. Gene expression profile identifies tyrosine kinase c-Met as a targetable mediator of anti-angiogenic therapy resistance. *Clin Cancer Res*. 2013 Mar 21. Epub ahead of print.
26. Wehrle-Haller B. Analysis of integrin dynamics by fluorescence recovery after photobleaching. *Methods Mol Biol*. 2007; 370:173–202. [PubMed: 17416995]
27. Liang CC, Park AY, Guan JL. *In vitro* scratch assay: a convenient and inexpensive method for analysis of cell migration *in vitro*. *Nat Protoc*. 2007; 2:329–33. [PubMed: 17406593]
28. Carbonell WS, Murase S, Horwitz AF, Mandell JW. Migration of perilesional microglia after focal brain injury and modulation by CC chemokine receptor 5: an *in situ* time-lapse confocal imaging study. *J Neurosci*. 2005; 25:7040–7. [PubMed: 16049180]
29. Hjelmeland AB, Wu Q, Heddleston JM, Choudhary GS, MacSwords J, Lathia JD, et al. Acidic stress promotes a glioma stem cell phenotype. *Cell Death Differ*. 2011; 18:829–40. [PubMed: 21127501]
30. Ljubimova JY, Fugita M, Khazenzon NM, Das A, Pikul BB, Newman D, et al. Association between laminin-8 and glial tumor grade, recurrence, and patient survival. *Cancer*. 2004; 101:604–12. [PubMed: 15274074]
31. Ljubimova JY, Fujita M, Khazenzon NM, Ljubimov AV, Black KL. Changes in laminin isoforms associated with brain tumor invasion and angiogenesis. *Front Biosci*. 2006; 11:81–8. [PubMed: 16146715]
32. Marshall JF, Rutherford DC, McCartney AC, Mitjans F, Goodman SL, Hart IR. Alpha v beta 1 is a receptor for vitronectin and fibrinogen, and acts with alpha 5 beta 1 to mediate spreading on fibronectin. *J Cell Sci*. 1995; 108 (Pt 3):1227–38. [PubMed: 7542669]
33. Clarke JL, Ennis MM, Yung WK, Chang SM, Wen PY, Cloughesy TF, et al. Is surgery at progression a prognostic marker for improved 6-month progression-free survival or overall survival for patients with recurrent glioblastoma? *Neuro Oncol*. 2011; 13:1118–24. [PubMed: 21813511]
34. Koh MY, Lemos R Jr, Liu X, Powis G. The hypoxia-associated factor switches cells from HIF-1 α - to HIF-2 α -dependent signaling promoting stem cell characteristics, aggressive tumor growth and invasion. *Cancer Res*. 2011; 71:4015–27. [PubMed: 21512133]
35. Park CC, Zhang HJ, Yao ES, Park CJ, Bissell MJ. Beta1 integrin inhibition dramatically enhances radiotherapy efficacy in human breast cancer xenografts. *Cancer Res*. 2008; 68:4398–405. [PubMed: 18519702]
36. Kim S, Bell K, Mousa SA, Varner JA. Regulation of angiogenesis *in vivo* by ligation of integrin alpha5beta1 with the central cell-binding domain of fibronectin. *Am J Pathol*. 2000; 156:1345–62. [PubMed: 10751360]

37. Grzesiak JJ, Tran Cao HS, Burton DW, Kaushal S, Vargas F, Clopton P, et al. Knockdown of the β 1 integrin subunit reduces primary tumor growth and inhibits pancreatic cancer metastasis. *Int J Cancer*. 2011; 129:2905–15. [PubMed: 21491421]
38. Huang C, Park CC, Hilsenbeck SG, Ward R, Rimawi MF, Wang YC, et al. β 1 integrin mediates an alternative survival pathway in breast cancer cells resistant to lapatinib. *Breast Cancer Res*. 2011; 13:R84. [PubMed: 21884573]
39. Lesniak D, Xu Y, Deschenes J, Lai R, Thoms J, Murray D, et al. Beta1-integrin circumvents the antiproliferative effects of trastuzumab in human epidermal growth factor receptor-2-positive breast cancer. *Cancer Res*. 2009; 69:8620–8. [PubMed: 19887601]
40. Damiano JS, Dalton WS. Integrin-mediated drug resistance in multiple myeloma. *Leuk Lymphoma*. 2000; 38:71–81. [PubMed: 10811449]
41. Hazlehurst LA, Damiano JS, Buyuksal I, Pledger WJ, Dalton WS. Adhesion to fibronectin via beta1 integrins regulates p27kip1 levels and contributes to cell adhesion mediated drug resistance (CAM-DR). *Oncogene*. 2000; 19:4319–27. [PubMed: 10980607]
42. Aoudjit F, Vuori K. Integrin signaling inhibits paclitaxel-induced apoptosis in breast cancer cells. *Oncogene*. 2001; 20:4995–5004. [PubMed: 11526484]
43. Pontiggia O, Sampayo R, Raffo D, Motter A, Xu R, Bissell MJ, et al. The tumor microenvironment modulates tamoxifen resistance in breast cancer: a role for soluble stromal factors and fibronectin through β 1 integrin. *Breast Cancer Res Treat*. 2012; 133:459–71. [PubMed: 21935603]
44. Oshita F, Kameda Y, Hamanaka N, Saito H, Yamada K, Noda K, et al. High expression of integrin beta1 and p53 is a greater poor prognostic factor than clinical stage in small-cell lung cancer. *Am J Clin Oncol*. 2004; 27:215–9. [PubMed: 15170136]
45. Lieberman DM, Laske DW, Morrison PF, Bankiewicz KS, Oldfield EH. Convection-enhanced distribution of large molecules in gray matter during interstitial drug infusion. *J Neurosurg*. 1995; 82:1021–9. [PubMed: 7539062]

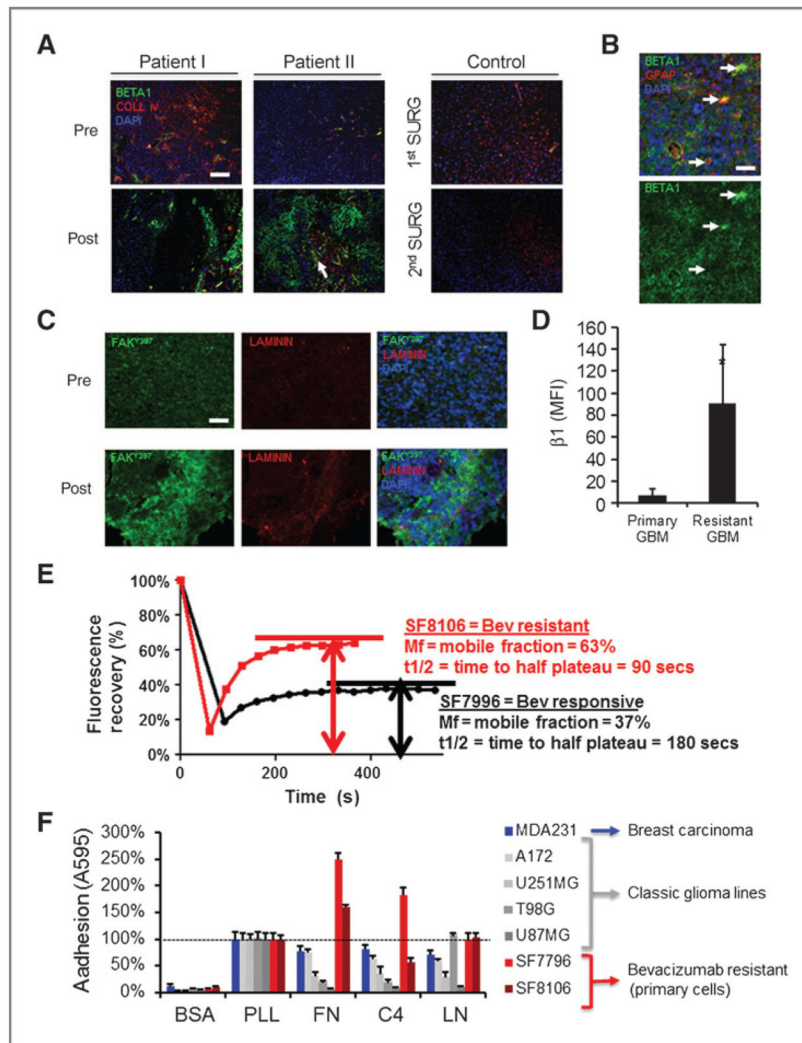
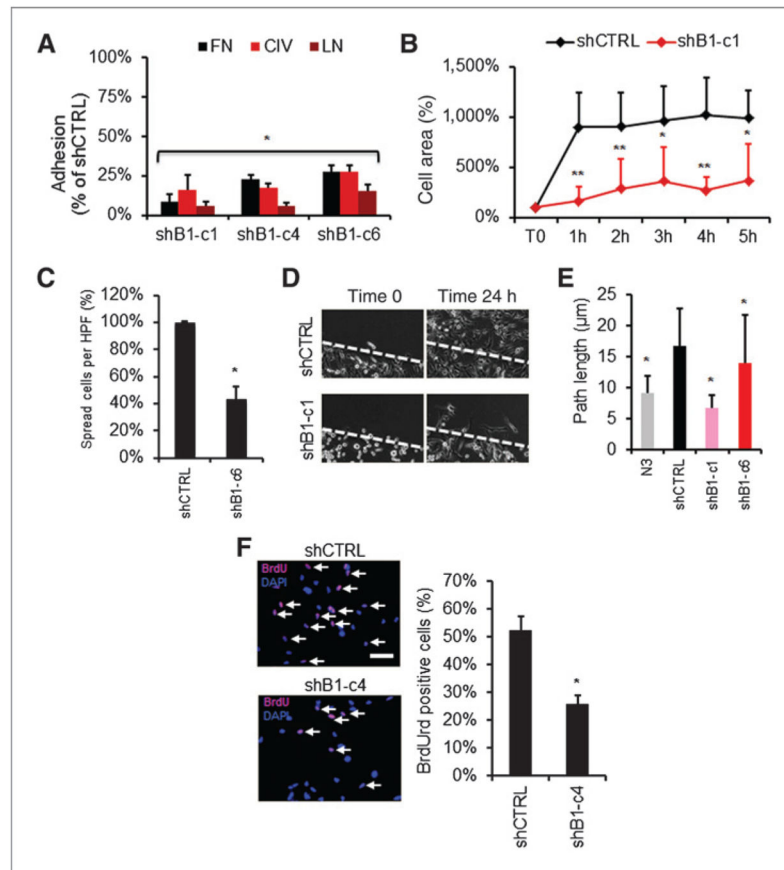


Figure 1.

$\beta 1$ integrin expression and bevacizumab resistance in glioblastoma. A, immunofluorescent staining for $\beta 1$ integrin (green); collagen IV, an endothelial marker (red); and 4', 6-diamidino-2-phenylindole nuclear counterstain in clinical specimens from 2 patients before and after development of bevacizumab resistance and a control patient at first and second surgery. Scale bar, 100 μm . B, high-powered view from another BRG shows $\beta 1$ integrin immunoreactivity in glioma cells including glial fibrillary acidic protein-positive cells (arrows). Scale bar, 50 μm . C, phosphorylated focal adhesion kinase (FAK^{Y397}, green) is enriched in post-bevacizumab tissues and correlated with ECM consistent with increased integrin activity. Scale bar, 120 μm . D, dissociated cells from resistant glioblastoma (GBM) have significantly higher $\beta 1$ integrin on flow cytometry than primary tumor cells (*, $P < 0.05$, t test). E, FRAP conducted on cells expressing $\beta 1$ -GFP fusion protein revealed more rapid $\beta 1$ integrin turnover in focal adhesions and a higher integrin mobile fraction in bevacizumab-resistant SF8106 cells than in bevacizumab-responsive SF7996 cells. Experiment was repeated 4 times, with distinct curves each time ($P < 0.001$, t test). F, BRG cells are more adherent to classical ECM proteins than several glioblastoma cell lines in

addition to the highly adherent MDA-MB-231 breast carcinoma (BSA, negative control; PLL, positive control; FN, fibronectin; C4, collagen type IV; LN, laminin). Data are mean \pm SD. See also Supplementary Fig. S2.

**Figure 2.**

$\beta 1$ integrin knockdown in resistant glioblastoma cells inhibits mesenchymal function. $\beta 1$ integrin knockdown clones are impaired in cell adhesion (A; *, $P < 0.01$, ANOVA with *post hoc* Dunnett test), dynamic cell spreading (B; *, $P < 0.05$, **, $P < 0.01$, ANOVA with *post hoc* Dunnett test), and percentage of spread cells (C; *, $P < 0.01$, Mann–Whitney test) on fibronectin. D and E, dynamic time-lapse analysis in a scratch wound assay shows impaired migration in knockdown clones versus control (*, $P < 0.05$, ANOVA with *post hoc* Dunnett test). $\beta 1$ integrin knockdowns show decreased proliferation as shown by BrdU immunofluorescence (F; *, $P < 0.01$, *t* test). Scale bar, 120 μm . Data are mean \pm SD. See also Supplementary Figs. S3 to S5.

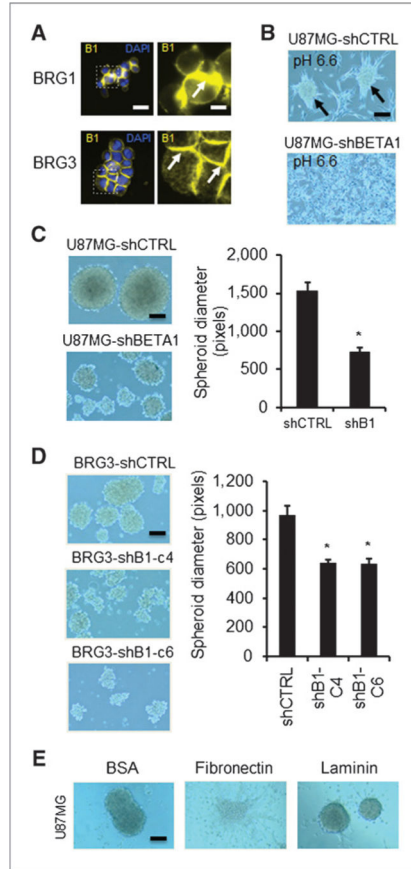


Figure 3.

β 1 knockdown in glioma cells inhibits spheroidal growth. A, immunofluorescence shows acutely enriched β 1 immunoreactivity at cell–cell contacts in 2 BRG lines in an *in vitro* aggregation assay. Scale bars, 30 and 10 μ m, respectively. B, β 1 knockdown in U87MG attenuates spheroid formation (arrows) in acidic media. Scale bar, 120 μ m. Formal spheroidal growth assay confirms impairment of spheroid diameter with β 1 knockdown in both U87MG (C; *, $P < 0.05$, t test; scale bar, 120 μ m) and BRG3 clones (D; *, $P < 0.05$, ANOVA with post-hoc Dunnett test; scale bar, 120 μ m). E, U87MG spheroids unravel when plated on fibronectin, but not BSA control substrate consistent with a β 1-mediated mechanism. Scale bar, 120 μ m. Data are mean \pm SD. See also Supplementary Fig. S6.

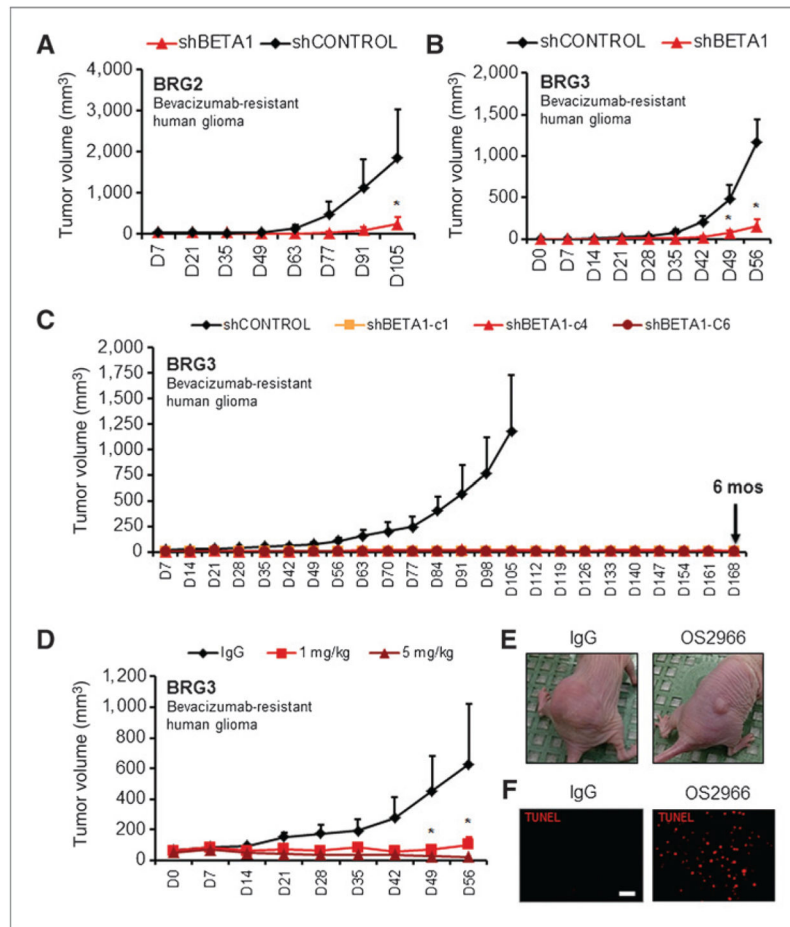


Figure 4.

$\beta 1$ integrin inhibition in BRG cells attenuates growth *in vivo*. Growth of polyclonal $\beta 1$ integrin knockdowns in a subcutaneous xenograft model was attenuated in both BRG2 (A; *, $P < 0.05$, ANOVA with *post hoc* Bonferroni test) and BRG3 (B; *, $P < 0.05$, ANOVA with *post hoc* Bonferroni test) lines. C, more than 90% knockdown of $\beta 1$ integrin in BRG3 clones prevents *in vivo* growth for up to 6 months. D and E, inhibitory anti-integrin antibody, OS2966, similarly inhibits growth of BRG3 cells *in vivo* at 1 or 5 mg/kg i.p. biweekly compared with control IgG (*, $P < 0.05$, ANOVA with *post hoc* Bonferroni test). F, 5 mg/kg of OS2966 induces more apoptosis in subcutaneous tumors than IgG. Scale bar, 100 μm . Data are mean \pm SEM. See also Supplementary Fig. S7A.

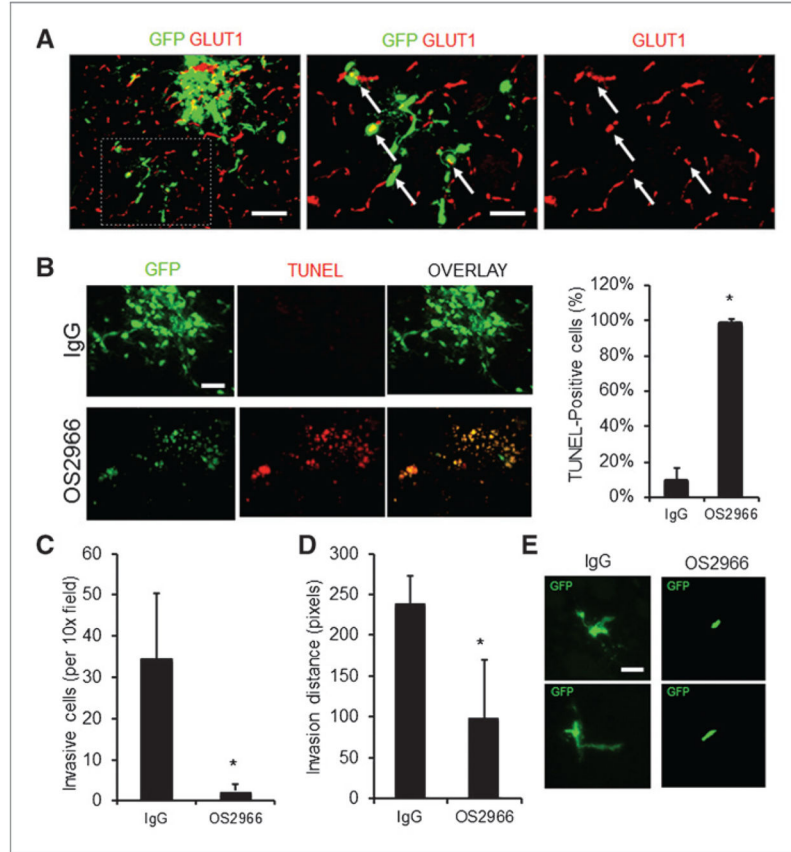


Figure 5.

OS2966 inhibits growth and invasion of orthotopically implanted BRG3 cells. A, low-power epifluorescent microscopy shows parenchymal invasion of BRG3 cells in IgG-treated control mice. Many instances of this invasion (>50%) occurred perivascularly consistent with vessel cooption (arrows). Scale bar, 120 μ m. B, induction of apoptosis after OS2966 versus IgG control mAb treatment (*, $P < 0.05$, t test). Scale bar, 120 μ m. Invasion of BRG3 cells in OS2966-treated mice was significantly attenuated as shown by number of invasive cells (C; *, $P < 0.05$, t test), invasion distance (D; *, $P < 0.05$, t test), and was supported by altered morphology of single invading cells including length and number of cellular processes (E). Scale bar, 50 μ m. Data are mean \pm SD. See also Supplementary Fig. S7.

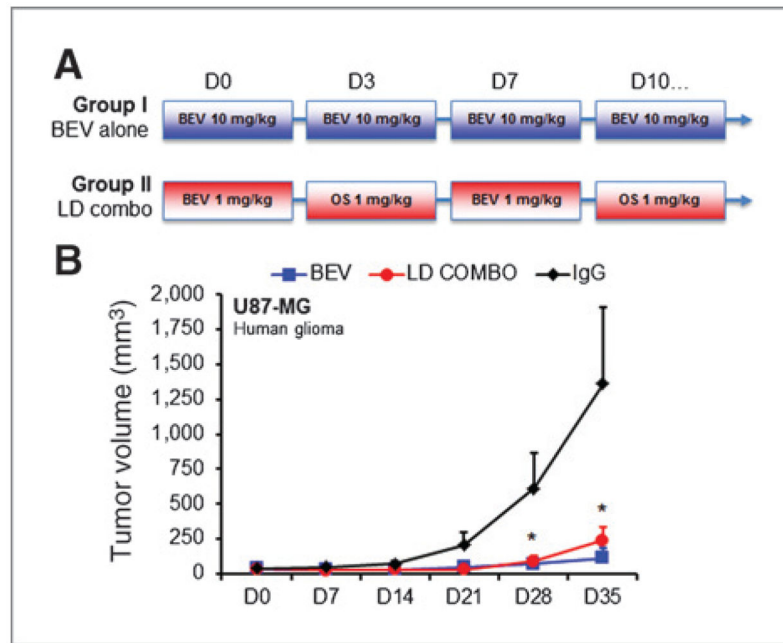


Figure 6. OS2966 potentiates efficacy of bevacizumab in a glioma model. A, study design of experimental groups with standard bevacizumab therapy at 10 mg/kg biweekly (group I, BEV) versus alternating bevacizumab and OS2966 at 1 mg/kg (group II, low-dose combo). B, inhibition of tumor growth with low-dose combo (group II) was equivalent to high-dose bevacizumab (group I) compared with IgG controls in subcutaneous U87MG xenografts (*, $P < 0.05$, ANOVA with *post hoc* Bonferroni test). Shown are mean \pm SEM.